

# Properties of Iron Powder Compressed Cores with Magnetite Thin Film Insulator

Pyungwoo Jang\*

College of Engineering, Cheongju University, Cheongju 28503, Korea

(Received 2 January 2020, Received in final form 6 February 2020, Accepted 6 February 2020)

It is very important to isolate soft magnetic particles electrically in order to reduce an eddy current loss of compressed cores. In this study, iron powders were oxidized in a mixed gas of  $N_2+H_2O$  at  $600^\circ C$  in order to encapsulate the powders completely by iron oxide and compressed into cores. The oxide film was analyzed to be  $Fe_3O_4$  by XRD as well as its color and grew linearly through oxidation. With increasing oxidation time, its permeability increased whereas the density decreased. The core, eddy current and hysteresis losses of the oxidized cores were much lower than those of the cores with insulating powders. It was confirmed that the  $Fe_3O_4$  film formed in a damp atmosphere could encapsulate the iron particles completely and ensured lower eddy current loss.

**Keywords :** compressed iron powder cores, magnetite film, dew point, oxidation of iron powder, core loss

## 마그네타이트 절연막을 가진 철압분 코어의 특성

장평우\*

청주대학교 공과대학, 충북 청주시 청원구 대성로 298, 28503

(2020년 1월 2일 받음, 2020년 2월 6일 최종수정본 받음, 2020년 2월 6일 게재확정)

압분코어에서 와전류손실을 줄이기 위해 자성분말을 완전히 절연시키는 기술은 매우 중요하다. 이 연구에서 수분무한 철분말을  $600^\circ C$ 의 질소와 수증기 혼합분위기에서 산화시킨 후 가압하여 압분코어를 제작하였다. 생성된 철산화물은 마그네타이트인 것이 XRD 분석과 색의 변화에서 확인할 수 있었다. 마그네타이트 막의 두께는 산화시간이 증가함에 따라 거의 직선적으로 증가하였다. 산화시간이 증가함에 따라 투자율은 증가하고 밀도는 감소하였다. 코어손실, 와전류손실 그리고 이력손실이 기존의 절연분말을 사용한 코어보다 월등히 낮았으며 이것은 마그네타이트의 비저항이 크지 않음에도 불구하고 철입자를 완전히 둘러싸는 것이 가능하기 때문이다.

**주제어 :** 철압분코어, 마그네타이트 필름, 이슬점, 철분말 산화, 코어손실

### I. Introduction

Compressed powder cores have been widely used for high frequency applications because of its low eddy current loss. Recently there has been great attention on such cores for future applications. It is because the cores have been known to be suitable for the power conditioning systems of hybrid vehicles, solar cell generators and so on. The merits of the cores are low loss at high frequency, low manufacturing cost, recyclability, high formability and so on.

The most important thing when manufacturing the cores is that each individual particle should be insulated electrically from its neighboring particles. Normally insulating films have been made by phosphate coating: MgO coating by gas-solid reaction, adding very fine insulating powders such as aluminum oxide, talc and etc to itself and others [1-7]. The as-compressed cores should be annealed in order to relieve the residual stress induced during compression. However, phosphate coating has shortcoming; it has maximum annealing temperature at around  $500^\circ C$  [8,9]. Such temperature is not high enough to allow the insulating powders to encapsulate the particles completely so that eddy current route cannot be cutoff sufficiently.

Iron oxide can be formed very easily on the surface of iron powders by using various chemical methods. Although

Fe<sub>3</sub>O<sub>4</sub> (magnetite) has the lowest electrical resistivity among iron oxides, it has been well known that the magnetite film is very dense and has high adhesive force to the matrix. Our previous study had showed that eddy current route could be totally cutoff in the powder core made of the particles perfectly coated by an 1 μm thick insulating film. This is possible only if the electrical resistivity of the film is about 10<sup>5</sup> times higher than that of the metallic particles [10]. Electrical resistivity of Fe<sub>3</sub>O<sub>4</sub> is around 10<sup>5</sup>-10<sup>6</sup> times higher than that of iron [11].

Iron has the highest saturation magnetization among ferromagnetic elements. Such property makes the iron powder be suitable as a good starting material of compressed cores if the particles are perfectly coated by an insulating film. It is well known that an Fe<sub>3</sub>O<sub>4</sub> passivation film forms on the surface by immersing the iron powders in nitric acid [12]. However, it is too thin to be used as an insulating film. The film can also be formed on the surface by oxidizing the iron powders in a damp atmosphere at a high temperature. Normally it is hard to use red-colored Fe<sub>2</sub>O<sub>3</sub> oxide as an insulating film which easily forms in the air because it is highly porous and hard to adhere to the iron powders.

In this study an Fe<sub>3</sub>O<sub>4</sub> film was formed on the Fe powders by oxidizing the powders in a damp atmosphere at 600 °C and the properties of the cores made of the Fe<sub>3</sub>O<sub>4</sub>-coated powders were investigated.

## II. Experimental Procedure

Water-atomized iron powders were sieved to have a diameter smaller than 180 μm. The morphology of the as-atomized iron powders is shown in the Fig. 1. In contrast

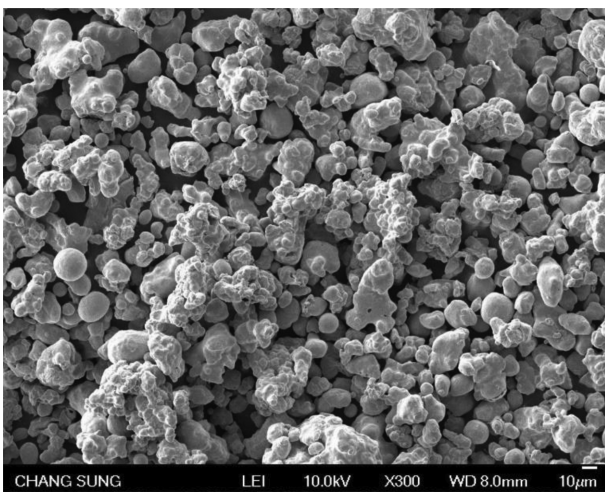


Fig. 1. SEM morphology of the water-atomized iron powders.

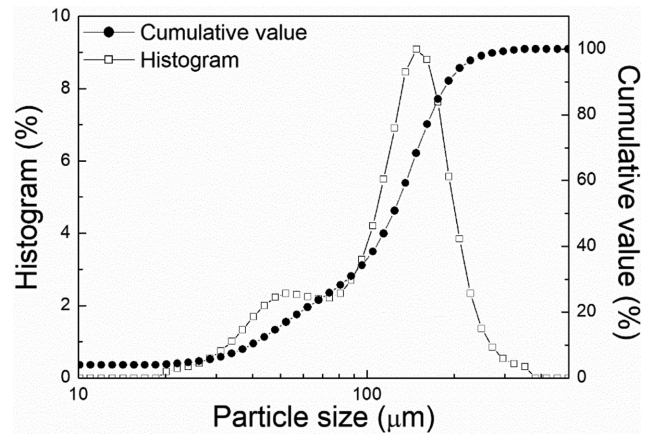


Fig. 2. Size distribution of the sieved iron powder.

to gas-atomized powders, the morphology of which was spherical, the morphology of the water-atomized powders was irregular. Size distribution of the powders is shown in Fig. 2. A diameter of the powders with most probable size was around 150 μm. The sieved iron powders were oxidized at 600 °C for up to 8 hours in N<sub>2</sub>+H<sub>2</sub>O mixed gas, the dew point of which was 70 °C. The oxidized powders were mixed with lubricant and then compressed into toroidal cores under a pressure of 1176 MPa; the inner and outer diameter of which were 7.6 and 12.7 mm, respectively. The compressed cores were annealed in vacuum better than 1 × 10<sup>-5</sup> torr at 700 °C for 1 hour and then furnace-cooled. The final cores are called oxidized cores hereafter. In order to check the growth rate of the oxide film a rectangular steel plate was oxidized in a same condition. For comparison, the compressed cores with powder insulators, the content of which was mostly talc and alumina, were manufactured. The powder insulator was added up to 3 wt.%. To reduce experimental errors, three cores were fabricated at a time in this experiment.

Core loss ( $P_{core}$ ) was measured using an Iwatsu SY-8232 AC loop tracer under a condition of maximum induction of 0.1 T and frequencies of 1, 10 and 50 kHz. The eddy current loss ( $P_{eddy}$ ) was calculated by subtracting hysteresis loss ( $P_{hyst}$ ) from core loss, for which DC hysteresis loops were measured under a condition of  $B_{max} = 0.1$  T. Permeability was measured at 100 kHz using HP 4284A impedance analyzer. For structural analysis, a Philips X'Pert x-ray diffractometer was used.

## III. Results and Discussion

The as-atomized iron powders turned black from grey after oxidation which meant the oxide film on the powders would be Fe<sub>3</sub>O<sub>4</sub>. In XRD measurement the oxide

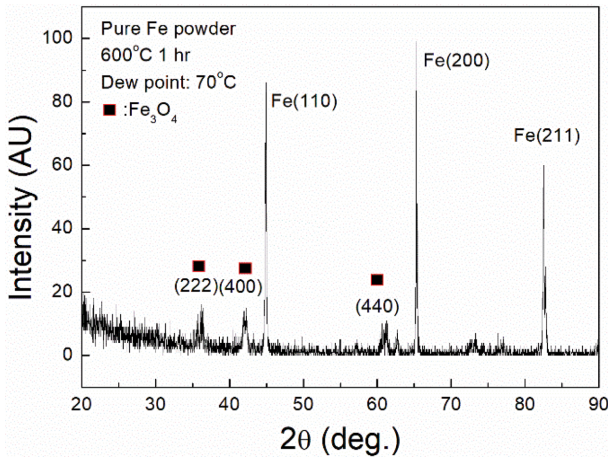


**Fig. 3.** (Color online) XRD pattern of the oxidized iron powders.

film formed on the surface of the iron powders was seemed to be  $\text{Fe}_3\text{O}_4$ . Possible iron oxides were  $\alpha\text{-Fe}_2\text{O}_3$  (hematite),  $\gamma\text{-Fe}_2\text{O}_3$  (maghemite) and  $\text{Fe}_3\text{O}_4$  (magnetite). Because maghemite and magnetite have spinel structure while hematite does not, it is easy to distinguish between the magnetic oxides and hematite in XRD patterns [13]. However, it is difficult to identify maghemite and magnetite using XRD patterns. The color of the magnetite and maghemite is black and dark brown, respectively. The color black of the oxidized powders indicates that the oxide film would be magnetite.

A low-carbon steel plate with rectangular shape was used to calculate the growth rate of the oxide film on the powders because it was difficult to measure the real surface area of the powders and then the thickness of the oxidized film. Color of the plate was black which meant that the oxide film was magnetite. The growth rate of the

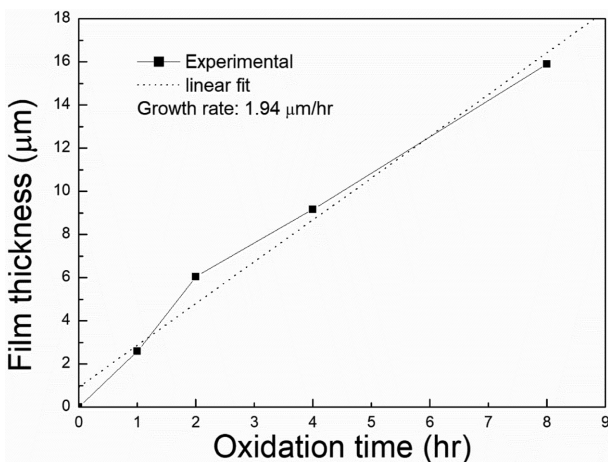


**Fig. 4.** Linear growth of the oxide film on the steel plate with oxidation time.

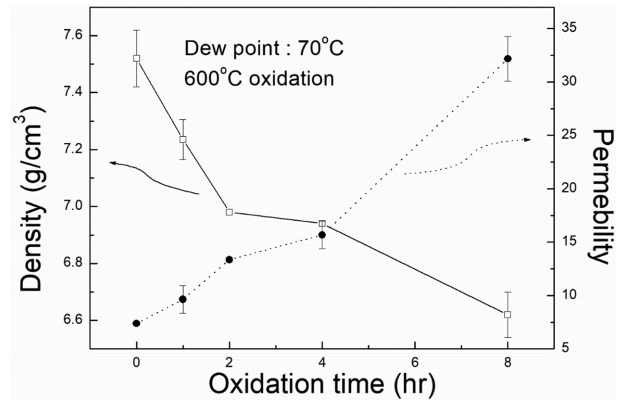


**Fig. 5.** Variation in density and permeability of the oxidized cores with oxidation time.

oxide on the plate was calculated by measuring mass increment after oxidation as shown in Fig. 4. The growth rate of the oxide film was about  $1.94 \mu\text{m/h}$  in the experimental condition and linear to oxidation time. It is well known that  $\text{Fe}_3\text{O}_4$  film also forms in concentrated nitric acid. However, the  $\text{Fe}_3\text{O}_4$  film is very thin due to passivation [12]. In this condition of damp atmosphere at  $600^\circ\text{C}$  the film grew continuously. However, the actual growth rate of the film on the powders would be different from  $1.94 \mu\text{m/h}$ . Oxide film are formed during water atomization of pure iron. However it was as thin as  $6\sim 7 \text{ nm}$  analyzed by x-ray photoelectron spectroscopy and Auger electron spectroscopy [14].

Fig. 5 shows the variation of the density and permeability of the oxidized cores with oxidation time. The  $\text{Fe}_3\text{O}_4$  film reduced the density of the oxidized cores. The low density of the cores would be due to the low density of the films as well as the low formability of the oxidized powders. The permeability of the oxidized cores has increased with oxidation time as shown in Fig. 5. In our previous FEM simulation where the ratio of the resistivity of Fe powder and  $1 \mu\text{m}$  thick insulating layer varied, the eddy current loss in the simulation had decreased with increasing ratio. Then the loss remained unchanged once the ratio reached  $10^5$  [10]. Thus, the increase of the permeabilities is due to the effective cutoff of eddy current route between adjacent particles in the cores. The density and permeability of the cores decreased from  $7.52$  to  $6.58 \text{ g/cm}^3$  and from  $7.4$  to  $32.2$  after  $8 \text{ h}$  oxidation, respectively.

Fig. 6 shows the variation of the dc hysteresis loops of the cores with oxidation time. With increasing oxidation time, the slopes of the loops near origin had decreased because of increased demagnetization of the oxidized powders which is due to the increased thickness of the oxide films. A shift of the hysteresis loops which is in-

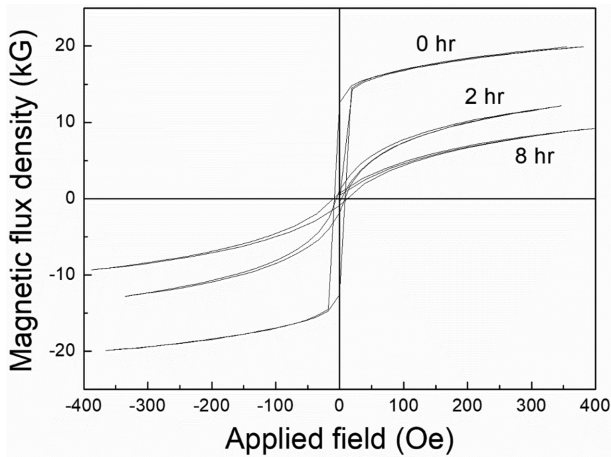


Fig. 6. DC hysteresis loops of the oxidized cores with oxidation time.

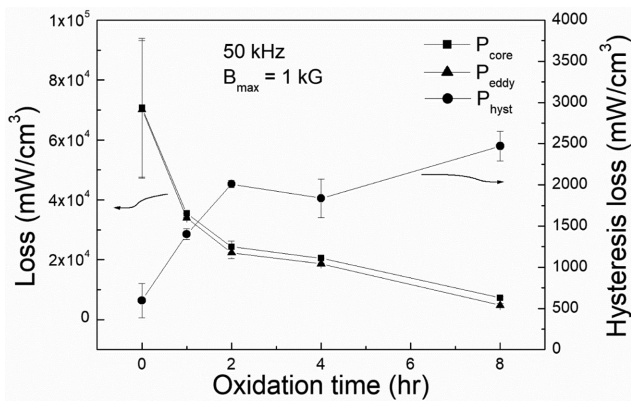


Fig. 7. Variations in core, hysteresis and eddy current losses of the oxidized cores with oxidation time.

teresting to observe was expected to occur in the cores composed of hard and soft magnetic materials.. However, no shift had been observed.

Fig.7 shows the variation of total, hysteresis and eddy current loss with oxidation time measured under a condition of 50 kHz and  $B_{max} = 0.1$  T. Hysteresis loss increased with oxidation time, one of the reasons for which seemed to be a reduction of the iron particle size after oxidation. Total loss decreased abruptly with oxidation time, which is due to the great reduction of the eddy current loss. The total loss of the oxidized iron cores was much higher than that of Fe-Si compressed cores, which is due to low resistivity of the pure iron particles. In Fig. 7 core losses of the cores were nearly same as eddy current loss of the cores because the frequency applied was as high as 50 kHz. It is well known that eddy current loss is proportional to the square of frequency.

Fig. 8 shows optical micrographs of the cores made of

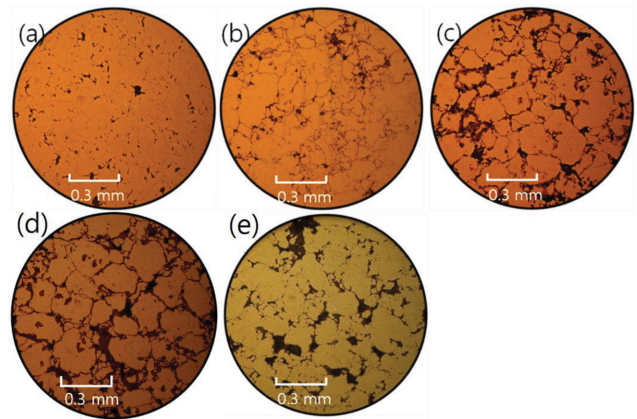


Fig. 8. (Color online) Optical micrographs of the oxidized cores with different oxidation time ((a) 0 h, (b) 1 h, (c) 4 h, (d) 8 h, (e) PI cores with 3% insulating powders).

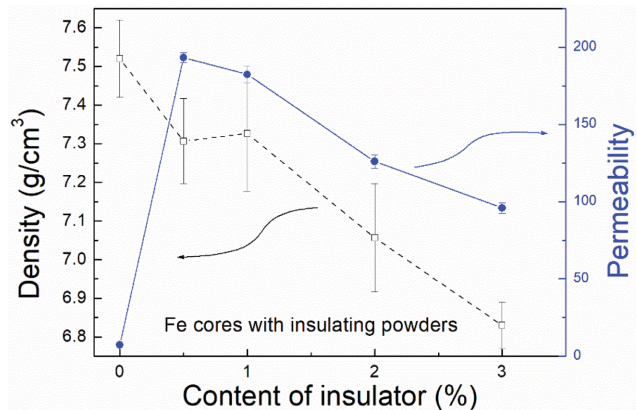


Fig. 9. (Color online) Variation in the density and permeability of the PI cores with content of insulating powders.

the powders with different oxidation time. In the micrograph of the core without oxide layer (a), interface between adjacent particles was not clearly seen. The interface became clear through oxidation. After eight hours of oxidation, it was more clear to be seen that the  $Fe_3O_4$  film completely encapsulated the iron particles.

In order to test the validity of the  $Fe_3O_4$  film as an excellent insulator, iron powders were mixed with insulating powders. The mixture had been compressed and then annealed under the same condition as that of the oxidized iron cores. These cores are called PI (powder insulator) cores hereafter. Insulating powder consisted of talc, alumina and lubricant powders. Fig. 9 shows variation of density and permeability of the PI cores with increasing amount of insulating powders. The density had decreased with increasing amount of the insulator at the same trend as shown in Fig. 5. The permeability had greatly increased with an addition of 0.5% insulating powders. However,



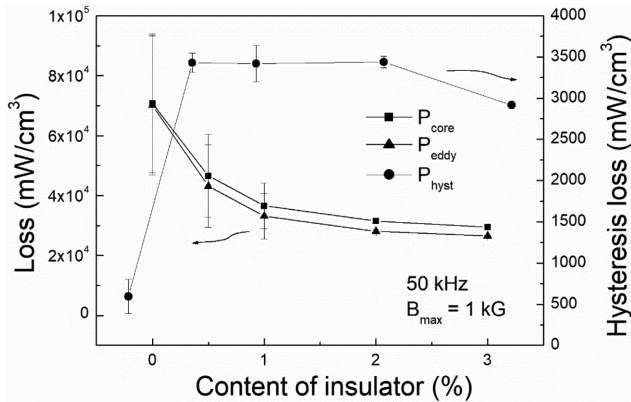


Fig. 10. Variation in total, hysteresis and eddy current losses of the PI cores with content of insulating powders.

permeability had gradually decreased with additional increasing amount of insulating powders. The reason for the decrease of permeability was same as that of the oxidized cores.

Fig. 10 shows variation of total, hysteresis and eddy current loss of the PI cores with content of insulator. Core loss of the PI cores had decreased greatly with content of the insulator and then decreased slightly beyond 1%. However, core loss of the cores was much larger than that of the oxidized iron cores. The loss of the oxidized core with 8 hours of oxidation was 7,286 mW/cm<sup>3</sup> while that of the PI core with 3% insulating powders was 29,430 mW/cm<sup>3</sup>. High core losses of the PI cores were due to high eddy current loss of the oxidized cores. Therefore, it can be seen that eddy current flowing across boundaries between adjacent particles had not been effectively cutoff

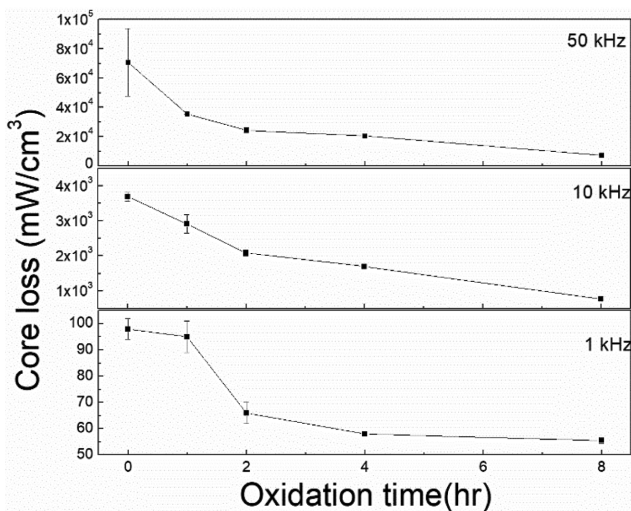


Fig. 11. Variation in the core losses of the oxidized cores with oxidation time at frequencies of 1, 10 and 50 kHz.

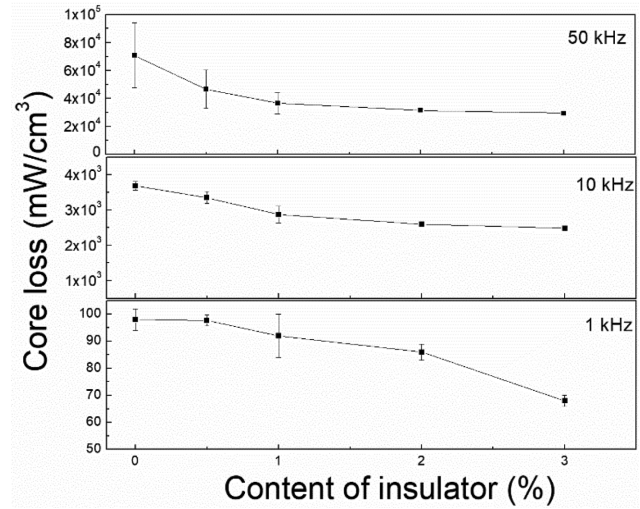


Fig. 12. Variation in core losses of the PI cores with content of insulating powders at frequencies of 1, 10 and 50 kHz.

inside the PI cores. An incomplete isolation of particles in the cores can be seen clearly in PI cores with 3 wt.% insulator as shown in Fig. 7(d).

Fig. 11 shows variations of core loss of the oxidized cores with oxidation time at frequencies of 1, 10, 50 kHz. At all frequencies core losses had decreased with oxidation time. After two hours the core losses decreased gradually through oxidation.

Fig. 12 shows variation of core losses of the PI cores with content of insulator at frequencies of 1, 10 and 50 kHz. At all frequencies core losses of the PI cores were much higher than those of the oxidized cores. The lowest core loss of the oxidized core at 1, 10 and 50 kHz were 55.5, 767 and 7,286 mW/cm<sup>3</sup> while those of the PI cores were 67, 2,490 and 29,430 mW/cm<sup>3</sup>.

#### IV. Conclusion

Water-atomized iron powders were oxidized in a damp atmosphere and then compressed into cores. The oxide film on the surface was revealed to be magnetite and the Fe<sub>3</sub>O<sub>4</sub> films on a steel plate grew almost linearly to oxidation time, the growth rate of which was 1.94 μm/h. As the oxidation time increased, the density and the permeability of the oxidized cores decreased and increased, respectively. The core loss and eddy current loss had decreased while hysteresis loss had increased through oxidation. Eddy current loss is the majority of the core loss at high frequency of 50 kHz. The core, eddy current and hysteresis losses of the PI cores were much higher than those of the oxidized cores. Although the resistivity of Fe<sub>3</sub>O<sub>4</sub> was much lower than that of alumina and other

oxides, this could greatly reduce the total loss of compressed Fe cores because the  $\text{Fe}_3\text{O}_4$  film could encapsulate Fe particles completely and thus reduce the eddy current loss.

### Acknowledgment

This work was supported by the research grant of Cheongju University in 2018.

### References

- [1] J. J. Zhong, J. G. Zhu, Z. W. Lin, Y. G. Guo, and J. D. Sievert, *J. Magn. Magn. Mater.* **290**, 1567 (2005).
- [2] J. J. Zhong, Y. G. Guo, J. G. Zhu, and Z. W. Lin, *J. Magn. Magn. Mater.* **299**, 29 (2006).
- [3] S. Gimenez, T. Lauwagie, G. Roebben, W. Heylen, and O. Van der Biest, *J. Alloys Compd.* **419**, 299 (2006).
- [4] Z. W. Lin and J. G. Zhu, *J. Magn. Magn. Mater.* **299**, 29 (2006).
- [5] D. H. Jang, T. H. Noh, G. B. Choi, Y. B. Kim and K. Y. Kim, *J. Appl. Phys.* **99**, 08F113 (2006).
- [6] P. Jang, B. Lee, and G. Choi, *J. Appl. Phys.* **103**, 07E743 (2008).
- [7] G. Uozumi, M. Watanabe, R. Nakayama, K. Igarashi, and K. Morimoto, *Materials Science Forum* **534-536**, 1361 (2007).
- [8] T. Madea, H. Toyoda, N. Igarashi, K. Hirose, K. Mimura, T. Nishikoa, and A. Ikejaya, *SEI Tech. Rev.* **60**, 3 (2005).
- [9] A. H. Taghvaei, H. Shokrollahi, and K. Janghorban, *J. Alloys Compd.* **481**, 681 (2009).
- [10] P. Jang and B. Lee, *IEEE Trans. Magn.* **45**, 2781 (2009).
- [11] J. M. D. Coey, *Magnetism and Magnetic Materials*, Cambridge University Press, New York, (2009) pp. 423.
- [12] D. Rahner, *Solid State Ionics* **86-88**, 865 (1996).
- [13] Md. S. Islam, Y. Kusumoto, Md.abdulla-Al-Mamun, H. Manaka, and Y. Horie, *Current Nanoscience* **8**, 811 (2012).
- [14] J. Wendel, R. Shvab, Y. Cao, E. Hryha, and L. Nyborg, *Surf. Interface Anal.* (2018).